Journal of Applied Physics

Energy condition of isothermal magnetoelectric switching of perpendicular exchange bias in Pt/Co/Au/Cr_2O_3/Pt stacked film

Cite as: J. Appl. Phys. **124**, 233902 (2018); https://doi.org/10.1063/1.5047563
Submitted: 09 July 2018 • Accepted: 30 October 2018 • Published Online: 18 December 2018

Thi Van Anh Nguyen, Yu Shiratsuchi, Shogo Yonemura, et al.

JOURNAL OF APPLIED PHYSICS **124**, 233902 (2018)

Energy condition of isothermal magnetoelectric switching of perpendicular exchange bias in Pt/Co/Au/Cr_2O_3/Pt stacked film

Thi Van Anh Nguyen,[1] Yu Shiratsuchi,[1,a)] Shogo Yonemura,[2] Tatsuo Shibata,[2] and Ryoichi Nakatani[1]
[1]*Department of Materials Science and Engineering, Graduate School of Engineering, Osaka University, Osaka 565-0871, Japan*
[2]*Advanced Technology Development Center, TDK Corporation, Chiba 272-0026, Japan*

(Received 9 July 2018; accepted 30 October 2018; published online 18 December 2018)

Energy condition for isothermal reversible magnetoelectric switching of exchange bias was investigated using Pt/Co/Au/Cr_2O_3/Pt stacked films with different thicknesses of the antiferromagnetic layer (t_{AFM}). We discussed the effective magnetic anisotropy energy of the antiferromagnetic layer (K_{AFM}^{eff}), the interface exchange coupling energy (J_{INT}), and the offset electric field (E_0). The dependence of K_{AFM}^{eff} on t_{AFM} suggested that the magnetic domain wall motion significantly influenced the switching of the electric-field-induced magnetization similar to an ordinal ferromagnet. Below 0.025 mJ/m^2, J_{INT} was equal to the exchange anisotropy energy (J_K), and above 0.025 mJ/m^2, J_{INT} exceeded J_K, suggesting that J_K is restricted by the magnetic domain wall energy. The dependence of E_0 on t_{AFM} revealed that E_0 mainly arose from the interfacial uncompensated antiferromagnetic moment. The obtained results suggest that the energetic interpretation of static switching of electric-field-induced magnetization in Cr_2O_3 was similar to that of the ordinary ferromagnetic materials. *Published by AIP Publishing.* https://doi.org/10.1063/1.5047563

I. INTRODUCTION

Exchange bias, which appears at the interface between an antiferromagnetic (AFM) and a ferromagnetic (FM) material, is visualized by a shift in the magnetic hysteresis loop away from the zero-magnetic field.[1–3] This shift is due to the unidirectional nature of the interfacial exchange coupling between the FM and AFM spins. The main purpose of the conventional exchange bias was to fix the FM magnetization to a certain direction in devices like spin-valve films.[4] The main limitation of this static use is that the isothermal control of the AFM spins is difficult. Recent progress in spintronics is breaking ground in this regard, and consequently, the dynamic use of exchange bias, i.e., switchable exchange bias, is possible.[5–14]

A promising way to achieve switchable exchange bias is to utilize magnetoelectric (ME) AFM materials because the net magnetization, which can be induced by an electric field (E), is controllable by a magnetic field (H).[5,6,8–16] Cr_2O_3 is a typical ME material, which retains its AFM characteristics above room temperature.[17,18] The highly significant ME-induced reversible switching of exchange bias at the FM/Cr_2O_3 interface was reported for bulk systems in a ME field cooling (MEFC) mode[5] and in an isothermal switching mode.[6] Since then, a significant research effort has been devoted to achieve ME switching of exchange bias in all-thin-film systems.[7–16] In the past four years, both switching modes have been achieved for FM/Cr_2O_3 stacked films. One of the most important fundamental requirements is the energy condition for the ME-induced switching. The energy condition for MEFC-driven switching has been discussed based on the analogy with magnetic-field-induced positive exchange bias.[15,16] Although the isothermal switching mode may be considered a more efficient manner not only for applying the application but also to elucidate the fundamental physics behind the switching, understanding of the switching energy associated with the isothermal switching mode is still insufficient. Previously, we reported the isothermal reversible ME switching of exchange bias, which established a characteristic relationship between the external H and E, and proposed the following equation to obtain the switching condition:[14]

$$\alpha\left(E+\frac{M_{AFM}}{\alpha}\right)H=-2K_{AFM}\mp\frac{J_{INT}}{t_{AFM}}, \tag{1}$$

where K_{AFM} is the magnetic anisotropy energy density of the AFM layer, J_{INT} is the interfacial exchange coupling energy per unit area, t_{AFM} is the thickness of the AFM layer, α is the ME coefficient of Cr_2O_3, and M_{AFM} is the uncompensated magnetization in the Cr_2O_3 layer. In this expression, the change in the sign of α was taken into account (see below). The sign of the second term depends on the switching direction: negative-to-positive (N-to-P) or positive-to-negative (P-to-N) switching of the polarity of the exchange bias. Equation (1) suggests that the energy condition for ME switching is directly related to t_{AFM}. Therefore, elucidating the t_{AFM} dependence of the energy condition affords a detailed understanding of ME switching. Herein, we show the energy condition for ME switching of the exchange bias, using a Pt/Co/Au/Cr_2O_3/Pt stacked film with various t_{AFM} values. Based on their threshold condition for switching, we discuss the prevailing factors of the parameters, i.e., K_{AFM}, J_{INT}, and M_{AFM}.

a)Author to whom correspondence should be addressed: shiratsuchi@mat.eng.osaka-u.ac.jp

II. EXPERIMENTAL METHODS

The Pt (1.2 nm)/Co (0.4 nm)/Au (0.5 nm)/Cr_2O_3 (t_{AFM})/Pt (20 nm) stacked films were prepared on α-Al_2O_3(0001) substrates by DC magnetron sputtering; t_{AFM} was varied between 115 nm, 130 nm, 147 nm, 169 nm, 173 nm, and 213 nm. Base pressure of the sputtering chamber was below 5×10^{-7} Pa. First, the Pt(111) buffer layer was deposited on the α-Al_2O_3(0001) substrate at 873 K. Then, the Cr_2O_3(0001) was deposited on the Pt(111) buffer layer at 773 K under the flow of an argon-oxygen gas mixture. The Au spacer layer, the FM Co layer, and the Pt capping layer were deposited at room temperature under an argon gas flow. The Au spacer layer was adopted to control the interfacial exchange coupling energy such that the exchange bias persisted up to the Néel temperature.[19] The above-mentioned crystalline orientation of the Pt and the Cr_2O_3 layers was characterized by *in situ*-reflection high-energy electron diffraction and X-ray diffraction. The actual value of t_{AFM} was determined by X-ray reflectivity (XRR) measurements. More details on sample preparation and structural characterization can be found in our previous paper.[19]

Magnetization measurements by a vibrating sample magnetometer (VSM, not shown) revealed that all the films studied possessed perpendicular magnetic anisotropy. Based on this, H was in a direction perpendicular to the film for all measurements; thus, the exchange bias studied here is directed perpendicularly to the film, i.e., the perpendicular exchange bias. For the perpendicular exchange bias, the exchange bias polarity can be detected based on an anomalous Hall effect (AHE). The AHE measurements were performed using the micro-fabricated Hall device (2-μm-wide and 40-μm-long) fabricated by photolithography, Ar ion-milling, and lift-off processes. The device with the measurement setup is schematically shown in Fig. 1. In our device, E, applied in a direction perpendicular to the film, was varied by changing the bias voltage applied across the Cr_2O_3(0001) layer between the bottom electrode (Pt buffer layer) and the top electrode (Pt cap layer). In this study, the positive direction of the field was defined as the direction from the bottom electrode to the top electrode of the device.

The ME switching of the exchange bias was performed as follows:

(1) The initial exchange bias state was set. The films were cooled from 310 K, i.e., above the Néel temperature (T_N) of bulk Cr_2O_3 (307 K)[17,18,20] to the measurement temperature (T_m) under a magnetic field of +6 kOe.
(2) The exchange bias polarity was switched at T_m; E and H were applied simultaneously. E was varied between −750 kV/cm (−11.25 V) and +1500 kV/cm (+22.5 V). The strength of H during E application was kept at either of varied between +60, +50, +40, and +30 kOe.
(3) The AHE loop was measured to check the exchange bias polarity; E was turned off, and then, AHE was measured as a function of H in the range of ±1.5 kOe. Typical AHE loops before and after the switching are shown in Fig. 1(b). The exchange bias field (H_{EB}) and the remanence ratio (M_R/M_S) were evaluated from the obtained AHE loop and were summarized as a function of E applied in process (2).

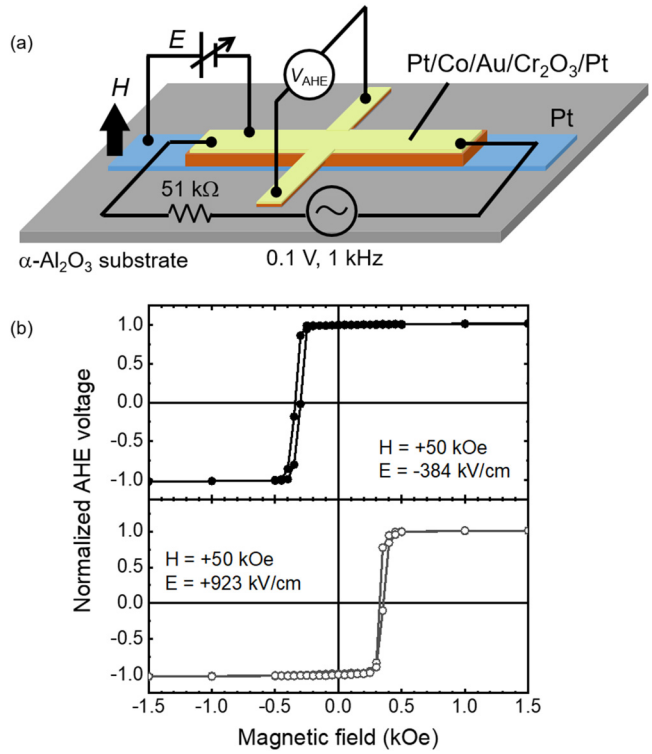

FIG. 1. (a) Schematic drawing of the Hall device with the anomalous Hall effect (AHE) measurement setup. (b) Typical AHE loops after the simultaneous application of E and H exhibiting the ME-induced switching of the exchange bias.

Since the thermal fluctuation of AFM spins, consequently, temperature dependences of K_{AFM} and α are significant at around T_N, the slight difference in T_N film-by-film would have a significant influence on the investigation of intrinsic t_{AFM} dependence when T_m was maintained at a certain temperature. Thus, we first determined T_N for all the films

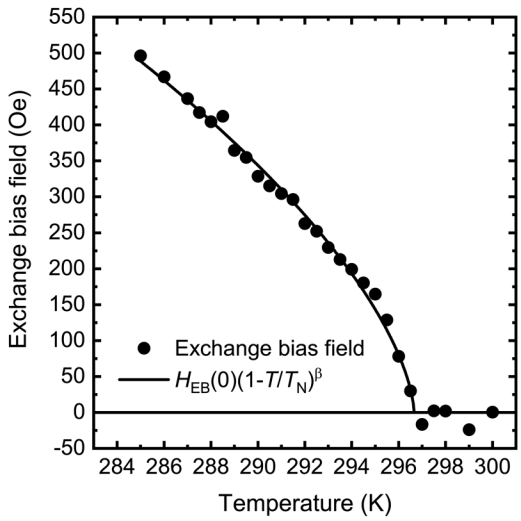

FIG. 2. Temperature dependence of the H_{EB} for the sample with the t_{AFM} of 130 nm. The closed circle and the line represent the experimental data and the fitting result using Eq. (2), respectively.

TABLE I. T_N, β, and T_m for all studied samples. The thickness of the Cr_2O_3 layer (t_{AFM}) was experimentally determined by XRR measurements. T_N and β were determined from the temperature dependence of the exchange bias field. T_m at which we investigated the t_{AFM} dependence of the switching energy was determined so that the reduced temperature T_m/T_N was the same ($T_m/T_N = 0.978$) for all studied samples.

t_{AFM} (nm)	T_N (K)	β	T_m (K)
115	293.6	0.72	287.2
130	296.5	0.62	290.0
147	293.5	0.65	287.0
169	297.1	0.77	290.6
173	300.4	0.77	293.8
213	296.7	0.59	290.2

studied based on the temperature dependence of H_{EB}.[21] Typical results of the temperature dependence of H_{EB} measured using the film with $t_{AFM} = 130$ nm are shown in Fig. 2. The reduction of H_{EB} near T_N could be quantified by a power-law with a critical exponent (β) and a scaling factor [$H_{EB}(0)$] as follows:

$$H_{EB}(T) = H_{EB}(0)\left(1 - \frac{T}{T_N}\right)^{\beta}. \quad (2)$$

T_N and β estimated using Eq. (2) for all the studied samples are summarized in Table I. For all the samples, β was in the range 0.59–0.77, which is close to the predicted[22–24] and experimental[25,26] values for the surface of three-dimensional (3D) Ising and 3D Heisenberg models. The t_{AFM} dependence of the ME switching condition was examined at the constant reduced temperature ratio of $T_m/T_N = 0.978$ to minimize the effect of temperature and sample dependence of α. T_m values for each sample are listed in Table I. In this study, in addition to t_{AFM} dependence, the temperature dependence of the ME switching condition was also investigated for more in-depth understanding, using the film with $t_{AFM} = 173$ nm where T_m was varied in the range 284–296 K. As can be seen in Eq. (1), for the estimation of K_{AFM} and J_{INT}, α is necessary, but it is difficult to determine the precise value of α, especially for the Cr_2O_3 thin film. In this paper, unless otherwise specified, we used α of the bulk Cr_2O_3[27,28] at the same T_m/T_N.

III. RESULTS AND DISCUSSIONS

The isothermal switching of the exchange bias by the simultaneous application of E and H was confirmed for the all studied samples to be typical AHE loops, as shown in Fig. 1(b). Note that only H below 60 kOe, i.e., without the application of E, could not induce the switching. For the isothermal switching with H only, an H higher than 80 kOe was required as we have previously reported.[29] Figure 3(a) shows the hysteresis loops showing the E dependence of H_{EB} and M_R/M_S for the sample with a t_{AFM} of 130 nm. The constant H during the application of E was +60 kOe. Reversible ME switching was observed, as in previous reports.[6,13,14] The threshold electric field (E_{th}) differed for positive and negative sides; the E_{th} values (or threshold voltage V_{th}) were +538.4±19 kV/cm (+7 ± 0.25 V) and −100.5 ± 7 kV/cm (−1.3 ± 0.1 V) for the positive and negative sides, respectively. Similarly, the E_{th} values at the other H strengths (+50 kOe, +40 kOe, +30 kOe) were also evaluated, and the change in E_{th} with $1/H$ (E_{th}-$1/H$ curve) was plotted, as shown in Fig. 3(b). The absolute value of E_{th} increased in direct proportion to $1/H$, meaning that the $E_{th}H$ product was constant, as expected from Eq. (1). The proportional relationship between E_{th} and $1/H$ is understood to mean that the energy gained by the ME effect is expressed by αEH.[28–30] In the following, we quantitatively discuss the origin of K_{AFM}^{eff}, J_{INT}, and the offset electric field E_0 obtained based on Eq. (1).

The slope for the N-to-P switching was opposite to that for the P-to-N switching. This is because for positive and negative exchange-biased states, the AFM order parameter, consequently, the sign of α was opposite. At the negative exchange biased state, the FM magnetization and the interfacial uncompensated AFM moment (boundary magnetization) are upward and downward, respectively, because of the antiferromagnetic interfacial exchange coupling.[31] Because the boundary magnetization couples with the AFM order parameter, α of the negative exchange-biased state is negative yielding that the slope of the E_{th}-$1/H$ curve for the N-to-P switching is positive. Oppositely, α of the positive exchange-biased state is positive yielding that the slope is negative.

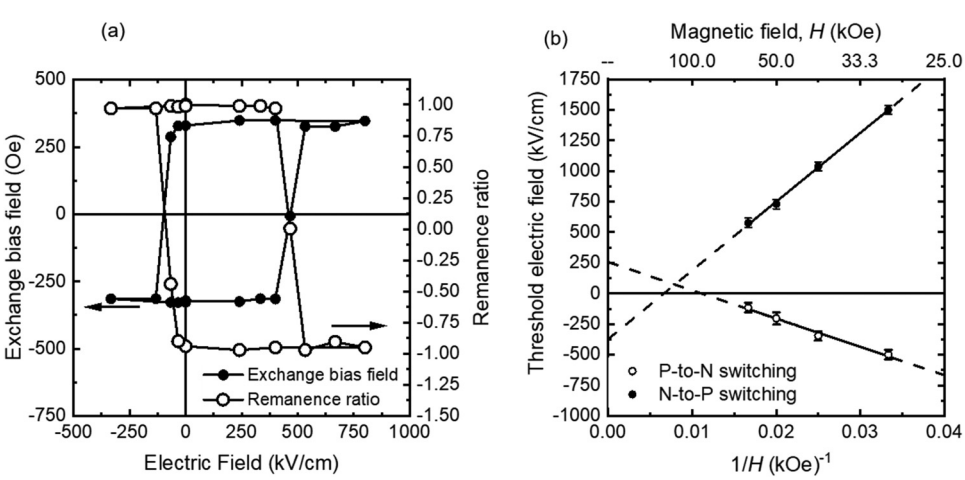

FIG. 3. (a) Electric field dependence of the H_{EB} and M_R/M_S for the sample with the t_{AFM} of 130 nm. During the electric field application, the magnetic field of +60 kOe was applied simultaneously to perform the ME switching process. Closed and open symbols represent H_{EB} and M_R/M_S, respectively. (b) Typical E_{th}-$1/H$ curve for the sample with the t_{AFM} of 130 nm. Closed and open symbols represent the experimental results for the N-to-P switching and the P-to-N switching, respectively. The lines in (b) represent the linear fitting of the experimental results.

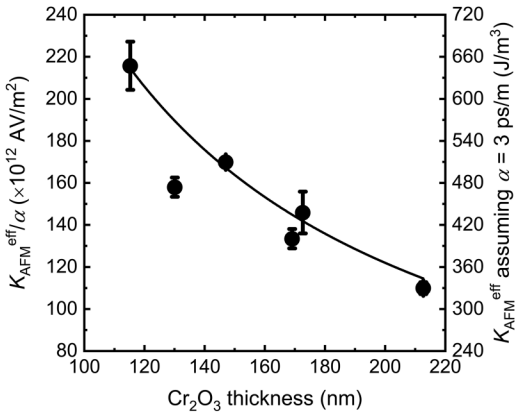

FIG. 4. t_{AFM} dependence of K_{AFM}^{eff} estimated from the E_{th}-1/H curve. The line is a guide for the eye. On the right axis, K_{AFM}^{eff} assuming $\alpha = 3$ ps/m was shown.

It should be noted that for both cases, αEH is always negative and this is reasonable because the reduction of αEH is a driving force to switch the AFM domain state. From Fig. 3(b), it can also be seen that the absolute values of the slopes were different. Equation (1) suggests that the average and the difference of the slopes of the E_{th}-1/H curves give K_{AFM}/α and J_{INT}/α, respectively. Figure 4 shows the t_{AFM} dependence of K_{AFM}^{eff}/α, which is seen to increase as t_{AFM} decreases. The estimated K_{AFM}^{eff}/α value is $1–2 \times 10^{-9}$ AV/m^2, which gives rise to K_{AFM}^{eff} in the middle of 10^2 J/m^3 assuming $\alpha = 3$ ps/m, approximately one order lower than the magneto-crystalline anisotropy energy density of the bulk Cr_2O_3 at the same T/T_N.[32] This is probably because Eq. (1) assumes coherent rotation, whereas the actual reversal proceeds via the nucleation and growth of the reversed AFM domain. The details of the magnetic domain wall motion during the ME-induced switching based on the direct observation of the magnetic domain, which strongly supports this discussion, will be reported elsewhere.[33]

One may assume that we can compare K_{AFM}^{eff} with the generally defined effective magnetic anisotropy of the FM film, K_U^{eff}. This is, however, difficult because of the different physical meaning of these two terms. K_U^{eff} of the FM film is expressed by

$$K_U^{eff} = K_U - \frac{N_d}{2\mu_0} M_S^2, \tag{3}$$

where N_d is the demagnetization factor and μ_0 is the susceptibility of vacuum. K_U^{eff} can be estimated from the anisotropy field H_K ($= K_U^{eff}/M_S$), which can be obtained from the magnetization curve along the magnetically hard axis. However, the K_{AFM}^{eff} presented here was estimated from the H_{EB} (M_R/M_S)-E curve along the magnetically easy axis (c-axis) of Cr_2O_3, more precisely, by using the cross-section point on the horizontal axis of the H_{EB} (or M_R/M_S)-E curve, i.e., the threshold E, E_{th}. E_{th} can be translated into the E-induced magnetization using the assumed α as $\alpha\, E_{th}$ at the remanent state. K_{AFM} was calculated from the averaged slope of the E_{th}-1/H curve [Fig. 3(b)], which corresponds to the Zeeman energy for $\alpha\, E_{th}$ at each applied H. In this meaning, the K_{AFM} estimated in this way is not the same as the usually defined magnetocrystalline anisotropy energy. In other words, the H_{EB} (M_R/M_S)-E curve is, in a way, the remanent magnetization curve of Cr_2O_3 along the c-axis (the magnetically easy axis) and K_{AFM}^{eff} represents the energy equivalent to the remanent coercivity. If the AFM spin reversal mode is perfectly coherent rotation, K_{AFM}^{eff} should be equal to the magneto-crystalline anisotropy energy of Cr_2O_3, K_{AFM} [the quantity shown in Eq. (1)]. However, in actual, K_{AFM}^{eff} is lower than K_{AFM} estimated from the bulk Cr_2O_3.[32] In addition, the increase of K_{AFM}^{eff} with decreasing t_{AFM} is equivalent to the increase of coercivity with decreasing thickness, which is well known as the result of the increase of the magnetic domain wall pinning energy. This result is also consistent with the above discussion that the prevailing factor of K_{AFM}^{eff} is the magnetic domain wall motion.

J_{INT} expresses the interfacial exchange coupling energy density. In its simplest form, as derived by Meiklejohn and Bean, J_{INT} is expressed as $J\boldsymbol{S}_{FM}\boldsymbol{S}_{AFM}$ and is equal to the exchange anisotropy energy density $J_K = H_{EB}M_S t_{FM}$ (M_S is the saturation magnetization of the FM layer and t_{FM} is the FM layer thickness). In this context, J_{INT} should correlate with J_K rather than t_{AFM}. As actually seen in the inset of Fig. 5(a), J_{INT}/α did not show a clear dependence on t_{AFM}. Instead, as shown in the main figure of Fig. 5(a), J_K was proportional to J_{INT}/α below about $J_K = 0.025$ mJ/m^2. Especially, assuming the α value as the bulk value at $T_m/T_N = 0.978$, ~3 ps/m,[27,28] J_{INT} and J_K were equal to each other as shown in the top horizontal axis of Fig. 5(a). When J_{INT} increased to ~0.05 mJ/m^2, J_K did not increase, but remained about 0.025 mJ/m^2. This can be interpreted based

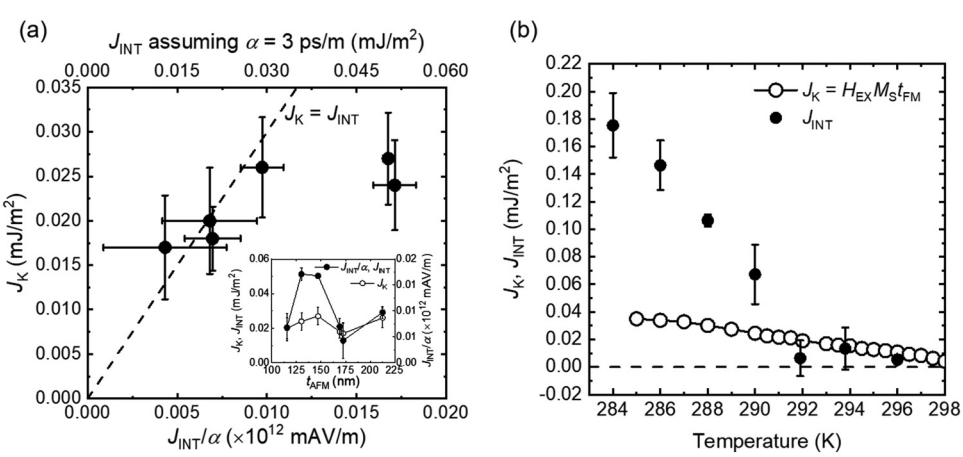

FIG. 5. (a) Correlation between J_{INT}/α and J_K. The dotted line represents $J_K = J_{INT}$. Inset shows the dependence of J_{INT}/α and J_K on Cr_2O_3 thickness. J_{INT} (the top horizontal axis of the main figure and the left axis of inset) was calculated assuming $\alpha = 3$ ps/m. One data point was collected for each sample measured at the corresponding measurement temperature listed in Table I. (b) Temperature dependence of J_K (open circle) and J_{INT} (closed circle). The inset of (a) represents the changes in J_{INT} and J_K with t_{AFM}. For the estimation of J_{INT}, α of the bulk Cr_2O_3 at each T_m/T_N was used.

on the magnetic domain wall model of the exchange anisotropy.[2,3,34] In this model, depending on the interface exchange parameter $\lambda = A_{12}/\xi \cdot 2(A \cdot K_{AFM})^{1/2}$ (A_{12} is the interfacial exchange stiffness, ξ is the interface spacing, A is the exchange stiffness of the AFM layer), J_K can be expressed as

$$J_K = \frac{A_{12}}{\xi} \quad \lambda \ll 1 \text{ (weak coupling)}, \tag{4-1}$$

$$J_K = 2\sqrt{AK_{AFM}} \quad \lambda \gg 1 \text{ (strong coupling)}. \tag{4-2}$$

Since the A_{12}/ξ is approximately $J\boldsymbol{S}_{FM}\boldsymbol{S}_{AFM}$ from the definition of the exchange stiffness, J_K in the weak interfacial exchange coupling regime should be equal to $J\boldsymbol{S}_{FM}\boldsymbol{S}_{AFM}$. In the strong interfacial exchange coupling regime, J_K is dominated by the magnetic domain wall energy of the AFM layer and does not follow $J\boldsymbol{S}_{FM}\boldsymbol{S}_{AFM}$ anymore. It should be mentioned that J_K is different between films in spite of the similar film structure except for t_{AFM}. This is probably because J_K of the FM/Cr_2O_3 stacked system highly depends on the crystalline quality of the Cr_2O_3 layer.[35,36] It is likely that the slight difference in the microstructure of the Cr_2O_3, e.g., the grain size, the in-plane crystallographic orientation, causes the significant change in J_K, in particular, in the strong J_{INT} regime. This may be because the magnetic domain wall pinning energy is affected by the structural defect in the AFM layer. At present, it is difficult to control J_K to the same value for the several films. The difference in J_K between samples in the weak J_{INT} regime may be because of the difference in the microstructure of the Au spacer layer, e.g., the island size. Because of the difference in the Au island size, the effective composition at the interface and the amount of the induced moment in Au can be altered; consequently, the interfacial exchange coupling J_{INT} can be different between films.

We further investigate the correlation of J_K and J_{INT} based on the temperature dependence. Obviously, most models of the exchange magnetic anisotropy assume the exchange bias when the FM magnetization is reversed, and this is valid for the estimation of J_K. However, in the case of the ME-induced switching of the exchange bias, i.e., for the estimation of J_{INT}/α, the E-induced magnetization in the AFM Cr_2O_3 is reversed while fixing the FM magnetization by the strong H above 30 kOe. Due in part to the very low thickness of the FM layer in our film, the formation of the magnetic domain in the FM layer is suppressed. Then, J_{INT} can be equal to A_{12}/ξ even in the strong coupling regime. In other words, the J_{INT} regime above ~0.03 mJ/m^2 is presumed to be the strong exchange coupling regime where J_{INT} and J_K can follow by Eqs. (4-1) and (4-2), respectively. We further investigate the correlation between J_K and J_{INT} from these temperature dependences. Figure 5(b) shows the temperature dependence of J_K and J_{INT} for the film with $t_{AFM} = 173$ nm. Above around 292 K, J_K and J_{INT} are almost equal. When the temperature decreased below around 292 K, J_K and J_{INT} start to deviate and J_K becomes lower than J_{INT}. At the bifurcation temperature, J_{INT} is 0.02–0.03 mJ/m^2, which roughly agrees with the criteria discussed in Fig. 5(a). In the usual in-plane exchange-biased system, J_{INT} is usually assumed independent of temperature. This is probably because the blocking temperature of these systems is far below T_N. In contrast, the measurements in this paper were carried out in the vicinity of T_N of Cr_2O_3 (see Table I). At the high T_m/T_N regime, the thermal fluctuation of S_{AFM} should be significant and J_{INT} can change with temperature. In this temperature regime, both J_{INT} and K_{AFM} change with temperature in the different fashion. Depending on the exquisite balance of J_{INT} and K_{AFM}, the exchange bias may vanish in the low temperature regime, which is in opposite manner to the usual case. Our previously observed high-temperature regeneration of the perpendicular exchange bias in Pt/Co/Pt/Cr_2O_3/Pt stacked films[37] may support the above discussion.

One may wonder that using the above results, we can estimate the magnetic domain wall width of the Cr_2O_3 layer and that the AFM domain wall is actually pinned in the AFM layer rather than slip through. As mentioned above, K_{AFM}^{eff} estimated here does not represent the magnetocrystalline anisotropy of the Cr_2O_3 layer, and thus it is difficult to calculate the domain wall width based on the above results. According to our previous report,[35,36] J_K of the film with the twinned Cr_2O_3 layer is more than 4 times higher than that of the film with the single crystalline Cr_2O_3 layer where J_K cannot exceed 0.1 mJ/m^2 at any temperature. This suggests that the magnetic domain wall pinning at the defect site such as grain boundary is one of the mechanisms of high J_K. In other words, the presence of the exchange bias exceeding 0.1 mJ/m^2 suggests that the domain wall pinning occurs in the Cr_2O_3 layer.

Next, we discuss the influence of M_{AFM} on the switching energy. In the limit of $1/H$ to zero in the E_{th}-$1/H$ curve [see Fig. 3(b)], the finite value of E_{th} was residual: the offset E, E_0. Defining E_0 phenomenologically as

$$\alpha(E - E_0)H = const. \tag{5}$$

As an origin of E_0, we can assume two possibilities: (1) the Schottly barrier caused by the difference in the work function between FM and Cr_2O_3 layers and (2) the uncompensated AFM moment that exhibits the ME effect. Defining E_0 as Eq. (5), E_0 is negative for the N-to-P switching and positive for the P-to-N switching, respectively, according to Fig. 3(b). Based on the Schottly barrier, it is difficult to change the sign of E_0 with respect to the switching direction, we consider the latter as the origin of E_0. By comparing Eq. (5) with Eq. (1), E_0 can be related to M_{AFM} in the Cr_2O_3 layer through

$$E_0 = -M_{AFM}/\alpha. \tag{6}$$

This expression is similar to that reported by Kosub *et al.*[38] The possible reason why M_{AFM} causes E_0 is bulk-site magnetization, such as the defect-induced finite magnetization located at the bulk site[38] M_{bulk} and/or the interfacial uncompensated AFM moments[10,14,31] $M_{interface}$, such as the surface magnetization.[39,40] Bulk and interface contributions to M_{AFM} can be included phenomenologically as follows:

$$M_{AFM} = M_{bulk} + \frac{M_{interface}}{t_{AFM}}. \tag{7}$$

Based on Eq. (7), M_{bulk} and $M_{interface}$ were estimated from the t_{AFM} dependence of E_0 shown in Fig. 6 where α was assumed as 3 ps/m. The relationship between E_0 and t_{AFM} is as expected and the fitting using Eq. (5) yielded $M_{bulk} = 3.8 \pm 2.5 \times 10^{-5}$ Wb/m^2 and $M_{interface} = 0.36 \pm 0.07\,\mu_B$/Cr. M_{bulk} is negligibly small, meaning that the defect-induced finite magnetization is negligible in our film. Taking into account the above-mentioned signs of α and E_0, M_{AFM} should be negative for both N-to-P and P-to-N switching; M_{AFM} is antiparallel to H in spite of the high H above +30 kOe. This is, however, consistent with our previous reports when the direction of the interfacial uncompensated AFM moment is determined by the interfacial exchange coupling with the FM moments.[31] Besides, the estimated $M_{interface}$ is of the same order as the interfacial uncompensated Cr moment estimated by the soft X-ray magnetic circular dichroism measurements,[31] $0.16\,\mu_B$. This correspondence suggests that the magnetic moment relevant to E_0 mainly originates from the interfacial uncompensated moments.

Another important point is that the interfacial uncompensated AFM moment can generate E. As discussed in our previous paper,[31] the interfacial uncompensated AFM moment is coupled with the FM moment. In this case, the interfacial uncompensated AFM moment behaves the same as the FM moment magnetically and is difficult to distinguish the FM moment. Then, one may wonder that the interfacial AFM moment is actually countable as the AFM moment to induce E_0. In our case, FM and AFM layers are metal and insulator, respectively. When the effective field acting on the interfacial AFM moment, e.g., the crystal field from the O^{2-} lattice, the exchange coupling with Cr^{3+} ion beneath the interface is different from either the FM moment or the Cr^{3+} ions at the bulk site. According to the phenomenological model of the ME effect of Cr_2O_3,[41] the ME effect is caused by the difference in the effective field acting on each sublattice. Hence, FM and interfacial AFM moments could be distinguishable in the viewpoint of the ME effect.

Finally, we mention the possible method to reduce the switching energy of the ME switching of the exchange bias. At the present stage, the switching energy is still high compared with the bulk system.[6] Based on the results shown here, the use of M_{AFM} may be effective to decrease the switching energy. As can be seen in Fig. 3(b), in the presence of M_{AFM} (more precisely E_0), E_{th} can be very small at the certain magnetic field, i.e., the cross-section point on the horizontal ($1/H$) axis. This approach has been already proposed for the MEFC driven switching[16] and it may be useful for the isothermal mode, as well. Even when M_{AFM} is used, the reduction of the slope of E_{th}-$1/H$, i.e., αEH is still important. This is because when the slope is large, the slight deviation of the applied H causes a significant increase of E_{th}. In other words, the operating margin of E is very low.

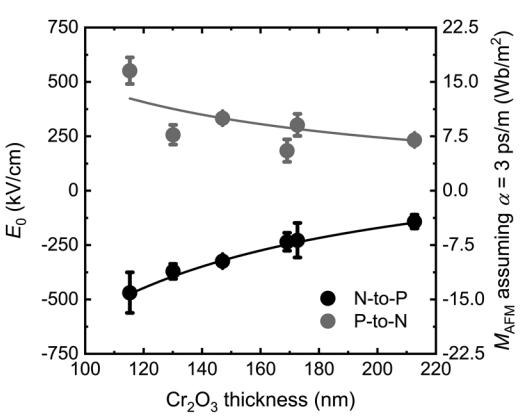

FIG. 6. t_{AFM} dependence of E_0. Gray and black circles represent E_0 for the N-to-P switching and the P-to-N switching, respectively. The solid lines are the fitting results using Eq. (7).

The results shown here suggest that the switching energy condition of Cr_2O_3 under finite E can be treated similarly to the ordinal FM (or ferrimagnet) layer in terms of the static switching. The dynamics of the E-induced magnetization of Cr_2O_3 also constitutes a nontrivial problem, while we implied that the simple model for the ferrimagnet was applicable to the magnetic domain wall motion of the E-induced magnetization.[13] For further understanding of the switching mechanism in both static and dynamic motion, direct observation of the switching process, for example, by observation of the magnetic domain is useful. This is now under investigation.

IV. SUMMARY

The ME switching of the exchange bias in Pt/Co/Au/Cr_2O_3/Pt stacked films with various Cr_2O_3 thicknesses was investigated in an isothermal, reversible manner. In particular, we focused on the quantitative analysis of the switching energy, mainly based on the dependence of the AFM layer thickness on the switching energy. K_{AFM}^{eff} of the Cr_2O_3 layer increased with decreasing thickness, implying that the switching energy was dominated by the magnetic domain wall pinning for the E-induced magnetization. The switching energy was asymmetric with respect to the switching direction. This asymmetry was explained by the unidirectional nature of the interfacial exchange coupling between FM and AFM spins. The comparison between J_K and J_{INT} suggested that J_{INT} could represent the inherent interfacial exchange coupling energy. The finite offset E in the limit of $1/H$ to zero was mainly caused by the interfacial uncompensated AFM moments, such as the surface magnetization. The obtained results suggest that the static switching energy condition of the E-induced magnetization of Cr_2O_3 is very similar to that of the ordinal FM (or ferrimagnet) materials.

ACKNOWLEDGMENTS

This work was partly supported by JSPS KAKENHI (Grant Nos. 17K18991, 16H03832, and 16H02389) and the Photonics Advanced Research Center (PARC) at Osaka University.

[1]W. H. Meiklejohn and C. P. Bean, Phys. Rev. **102**, 1413 (1956).
[2]J. Nogué and I. K. Schuller, J. Magn. Magn. Mater. **192**, 203 (1999).
[3]A. E. Berkowitz and K. Takano, J. Magn. Magn. Mater. **200**, 552 (1999).
[4]B. Dieny, V. S. Speriosu, S. Metin, S. S. P. Parkin, B. A. Gurney, P. Baumgart, and D. R. Wilhoit, J. Appl. Phys. **69**, 4774 (1991).
[5]P. Borisov, A. Hochstrat, X. Chen, W. Kleemann, and C. Binek, Phys. Rev. Lett. **84**, 117203 (2005).

[6]X. He, Y. Wang, N. Wu, A. N. Caruso, E. Vescovo, K. D. Belashchenko, P. A. Dowben, and C. Binek, Nat. Mater. **9**, 579 (2010).
[7]S. M. Wu, S. A. Cybart, P. Yu, M. D. Rossell, J. X. Zhang, R. Ramesh, and R. C. Dynes, Nat. Mater. **9**, 759 (2010).
[8]T. Ashida, M. Oida, N. Shimomura, T. Nozaki, T. Shibata, and M. Sahashi, Appl. Phys. Lett. **104**, 152409 (2014).
[9]K. Toyoki, Y. Shiratsuchi, T. Nakamura, C. Mitsumata, S. Harimoto, Y. Takechi, T. Nishimura, H. Nomura, and R. Nakatani, Appl. Phys. Express **7**, 114201 (2014).
[10]K. Toyoki, Y. Shiratsuchi, A. Kobane, S. Harimoto, S. Onoue, H. Nomura, and R. Nakatani, J. Appl. Phys. **117**, 17D902 (2015).
[11]T. Ashida, M. Oida, N. Shimomura, T. Nozaki, T. Shibata, and M. Sahashi, Appl. Phys. Lett. **106**, 132407 (2015).
[12]K. Toyoki, Y. Shiratsuchi, A. Kobane, C. Mitsumata, Y. Kotani, T. Nakamura, and R. Nakatani, Appl. Phys. Lett. **106**, 162404 (2015).
[13]T. V. A. Nguyen, Y. Shiratsuchi, and R. Nakatani, Appl. Phys. Express **10**, 083002 (2017).
[14]T. V. A. Nguyen, Y. Shirastuchi, A. Kobane, S. Yoshida, and R. Nakatani, J. Appl. Phys. **122**, 073905 (2017).
[15]T. Nozaki, M. Al-Mahdawi, S. P. Pati, S. Ye, Y. Shiokawa, and M. Sahashi, Jpn. J. Appl. Phys. **56**, 07302 (2017).
[16]M. Al-Madwawi, S. P. Pati, Y. Shiokawa, S. Ye, T. Nozaki, and M. Sahashi, Phys. Rev. B **95**, 144423 (2017).
[17]D. N. Astrov, Sov. Phys. JETP **11**, 708 (1960).
[18]V. J. Folen, G. T. Rado, and E. W. Stadler, Phys. Rev. Lett. **6**, 607 (1961).
[19]Y. Shiratsuchi, W. Kuroda, T. V. A. Nguyen, Y. Kotani, K. Toyoki, T. Nakamura, M. Suzuki, K. Nakamura, and R. Nakatani, J. Appl. Phys. **121**, 073902 (2017).
[20]T. G. MacGuire, E. J. Scott, and F. H. Grannis, Phys. Rev. **102**, 1000 (1956).
[21]D. Lederman, J. Nogués, and I. K. Schuller, Phys. Rev. B **56**, 2332 (1999).
[22]K. Binder and P. C. Hohenberg, Phys. Rev. B **9**, 2194 (1974).
[23]K. Binder and D. P. Landau, Phys. Rev. Lett. **52**, 318 (1984).
[24]D. P. Landau and K. Binder, Phys. Rev. B **41**, 4633 (1990).
[25]L. Fallarino, C. Binek, and A. Berger, Phys. Rev. B **91**, 214403 (2005).
[26]P. Borisov and W. Kleeman, J. Appl. Phys. **110**, 033917 (2017).
[27]A. Iyama and T. Kimura, Phys. Rev. B **87**, 180408R (2013).
[28]P. Borisov, T. Ashida, T. Nozaki, M. Sahashi, and D. Lederman, Phys. Rev. B **93**, 174415 (2016).
[29]Y. Shiratsuchi, K. Wakatsu, T. Nakamura, H. Oikawa, S. Maenou, Y. Narumi, K. Tazoe, C. Mitsumata, T. Kinoshita, H. Nojiri, and R. Nakatani, Appl. Phys. Lett. **100**, 262413 (2012).
[30]T. J. Martin and J. C. Anderson, IEEE Trans. Magn. **2**, 446 (1966).
[31]Y. Shiratsuchi, H. Noutomi, H. Oikawa, T. Nakamura, M. Suzuki, T. Fujita, K. Arakawa, Y. Takechi, H. Mori, T. Kinoshita, M. Yamamoto, and R. Nakatani, Phys. Rev. Lett. **109**, 077202 (2012).
[32]S. Foner, Phys. Rev. **130**, 183 (1963).
[33]Y. Shiratsuchi, S. Watanabe, H. Yoshida, N. Kishida, R. Nakatani, Y. Kotani, K. Toyoki, and T. Nakamura, "Observation of the magnetoelectric reversal process of the antiferromagnetic domain," (unpublished).
[34]D. Mauri, H. C. Siegmann, P. S. Bagus, and E. Kay, J. Appl. Phys. **62**, 3047 (1987).
[35]Y. Takechi, K. Wakatsu, T. Nishimura, Y. Shiratsuchi, and R. Nakatani, in *International Conference of the Asian Union of Magnetics Societies* (2012), 4pPS-57.
[36]Y. Shiratsuchi, Y. Nakano, N. Inami, T. Ueno, K. Ono, R. Kumai, R. Sagayama, and R. Nakatani, J. Appl. Phys. **123**, 103902 (2018).
[37]Y. Shiratsuchi, Y. Takechi, K. Toyoki, Y. Nakano, S. Onoue, C. Mitsumata, and R. Nakatani, Appl. Phys. Express, **6**, 123004 (2013).
[38]T. Kosub, M. Kopte, R. Hühne, P. Appel, B. Shields, P. Maltinsky, R. Hübne, M. O. Liedke, J. Fassbender, O. G. Schimidt, and D. Makarov, Nat. Commun. **8**, 13985 (2017).
[39]A. F. Andreev, JETP Lett. **63**, 758 (1996).
[40]K. D. Belashchenko, Phys. Rev. Lett. **105**, 147204 (2010).
[41]T. H. O'Dell, *The Electrodynamics of Magneto-Electric Media* (North-Holland Publishing Company, Amsterdam, 1970), pp. 238–242.